OPEN ACCESS
JOURNAL OF ADVANCED DIELECTRICS
Vol. 11, No. 2 (2021) 2150011 (12 pages)

DOI: 10.1142/S2010135X21500119

Dielectric spectroscopy and structural characterization of nano-filler-loaded epoxy resin

S. G. Thakor, V. A. Rana*, H. P. Vankar and T. R. Pandit

Department of Physics, School of Sciences, Gujarat University
Ahmedabad 380009, Gujarat, India

**varana@gujaratuniversity.ac.in*

Received 1 February 2021; Revised 6 March 2021; Accepted 11 March 2021; Published 7 April 2021

This work outlines the characterization of epoxy resin [Bisphenol A-(epichlorhydrin): epoxy] and hardener [*N*(3-dimethylaminopropyl)-1,3-propylenediamine] with various inorganic nano-fillers. Dielectric characterizations of epoxy, hardener, neat epoxy (epoxy + hardener) and nano-epoxy (nano-filler + neat epoxy) composites loaded with 1 wt.% of inorganic nano-fillers (SiO_2, Al_2O_3, TiO_2 and ZnO) were carried out using precision LCR meter, over the frequency range of 1 kHz–2 MHz at a constant temperature of 300.15 K. The structural information of nano-fillers, neat epoxy and nano-epoxy composites was understood by Fourier transform infrared spectroscopy and by XRD. Moreover, hardness and shear strength (shear punch) were also determined in order to gain additional information about the mechanical properties of epoxy composite. Influence of inorganic nano-fillers on the dielectric properties, structural chemistry and mechanical properties of neat epoxy composite is discussed thoroughly in this study.

Keywords: Epoxy resin; nano-fillers; dielectric relaxation spectroscopy; FTIR; mechanical properties; XRD.

1. Introduction

During the last decade epoxy resin had been the intense research focus for many researchers, because it offers excellent electrical, mechanical, chemical and thermal properties.[1–12] These properties can further be improved by adding nano-filler in the epoxy resin. In general, 0.1–5-wt.% nano-filler-loaded polymer nano-composites have been extensively investigated in view of their thermal, mechanical, physical and dielectric properties.[13–15] Both the types of enhanced and attenuated dielectric properties, i.e., dielectric constant, AC conductivity as well as mechanical properties, i.e., hardness and shear strength, of epoxy nano-composite compared to neat epoxy resin have been reported.[16–20] In our previous research papers, we have reported the dielectric/electrical properties of neat epoxy resin and different weight percentages of nano-filler-loaded epoxy resin over the frequency span of 1 kHz–2 MHz at room temperature (300.15 K). These studies suggested that the presence of nano-filler can lead to higher or lower relative permittivity and AC conductivity compared to those of neat epoxy resin, depending on the type and concentration of nano-filler.[21–23]

The usage of inorganic nano-fillers SiO_2, ZnO, Al_2O_3 and TiO_2 appears promising for the reinforcement of epoxy resin.[24] Fothergill *et al*.[16] studied the dielectric properties of ZnO–, Al_2O_3– and TiO_2-substituted epoxy composite using Stern–Gouy–Chapman interaction zone theory and concluded that the size of nano-filler appears to be important in altering the dielectric properties of neat epoxy. Singha and Thomas[15] reported that dielectric permittivity of nano-composite strongly depends on the concentration and permittivity of nano-filler. Wetzel *et al*.[25] reported improved stiffness, impact energy and failure strain at low filler concentration by the addition of aluminum oxide nano-filler into epoxy resin. Ng *et al*.[26] added TiO_2 nano-filler in epoxy resin and observed improved strain-to-failure characteristic. Clear understanding of the effect of type, size and concentration of nano-filler on epoxy resin system and on cure reactions of the stoichiometric mixtures of epoxy and hardener is yet missing. So, the aim of this investigation is to gain more information about the effect of adding SiO_2, ZnO, Al_2O_3 and TiO_2 nano-sized inorganic fillers in a fixed proportion on the dielectric, electrical, structural and mechanical properties of epoxy resin.

In this paper, we report the complex permittivities of epoxy, hardener, neat epoxy and 1 wt.% of nano-particle-loaded epoxy (nano-epoxy) composites over the frequency range of 1 kHz–2 MHz at a constant temperature of 300.15 K. The Fourier transform infrared spectroscopy (FTIR) spectra of neat epoxy and nano-epoxy composites are reported and discussed. In this work, the effect of addition of 0.5-, 1- and 1.5-wt.% nano-filler into the neat epoxy on the mechanical properties (hardness and shear strength) is discussed.

*Corresponding author.

Moreover, the structural morphologies of nano-fillers, neat epoxy and nano-epoxy composites are reported using X-ray diffraction (XRD).

2. Materials and Methods

2.1. *Sample preparation*

The epoxy resin [Bisphenol A-(epichlorhydrin): epoxy] and hardener [*N*(3-dimethylaminopropyl)-1,3-propylenediamine] were procured from Hindustan Ciba Geigy, Ltd., Mumbai, India, and were used for dielectric measurements without further purification. For the preparation of nano-epoxy composites, we procured high-purity grades of commercially available uncoated nano-filler-size compounds of SiO_2 (average particle size: 20 nm; Otto Chemie Private Limited, Mumbai, India; product code: SO 110), ZnO [average particle size: 30 nm; Sisco Research Laboratories Pvt., Ltd. (SRL), Mumbai, India; product code: 91140(2640103)], TiO_2 [average particle size: 50 nm; SRL, Mumbai, India; product code: 90885(2040262)] and Al_2O_3 [average particle size: 30 nm; SRL, Mumbai, India; product code: 75964(0140408)]. A neat epoxy sample was prepared by mixing 100th part of wt.% of the epoxy homogenously with 80th part of wt.% of hardener. Similarly, for preparing nano-epoxy composite, 1 wt.% of nano-fillers were dispersed with care into neat epoxy with manual mixing method following the procedure described in Refs. 27–29. Finally, the uniformly mixed dough (neat epoxy filled with nano-filler) was slowly decanted into the plastic molds, coated earlier with wax. The composites were casted in this mold of 2.5-cm diameter and 4-mm thickness in order to get disc-type specimens. Prepared samples were kept under vacuum desiccation prior to utilization for the experiment.

2.2. *Experimental techniques*

The dielectric measurements of Bisphenol A-epichlorhydrin and *N*(3-dimethylaminopropyl)-1,3-propylenediamine in liquid state were performed using Agilent E4980A precision LCR meter along with the liquid test fixture designed by Rana *et al*.[30] over the frequency range of 1 kHz–2 MHz. Prior to initiating the experiment, calibration technique as mentioned in Agilent's manual[31] was followed. For the dielectric measurements of neat epoxy and nano-epoxy composites in pellet form over the frequency range of 1 kHz–2 MHz, Agilent E4980A precision LCR meter with solid dielectric test fixture Agilent 16451B was used.[32] Utilizing the experimental dielectric data, other electrical properties were determined and detailed analysis of evaluated parameters for all the samples was carried out.

Information about the surface chemistry of nano-fillers and functional groups associated with epoxy resin were obtained from the FTIR spectra, which were determined using Agilent Cary 630 FTIR spectrometer. Mechanical properties like hardness and shear strength were measured using Blue Steel Shore D hardness tester according to IS 13360 standards[33] and Dutron UTM testing machine according to IS 2036 standards,[34] respectively. Moreover, the XRD spectra of all the nano-filler, neat epoxy and nano-epoxy composites were measured using a Rigaku-make diffractometer[35] with the Cu source (Cu-Kα = 0.154 nm, 40 kV, 45 mA) and data was taken for the angular range of 10–70° (2θ, for all nano-filler composites) and 5–70° (2θ, for neat epoxy and nano-epoxy composites). All measurements were carried out at 300.15-K temperature.

2.3. *Evaluation of dielectric and electrical properties*

The real part (ε'), i.e., dielectric constant, and imaginary part (ε''), i.e., dielectric loss, of the complex permittivity $\varepsilon^*(f)$ and loss tangent (tan δ) are evaluated using the following equations, respectively, for all prepared samples:

$$\varepsilon^*(f) = \varepsilon' - j\varepsilon'' = \alpha\left(\frac{C_p}{C_o} - j\frac{1}{\omega C_o R_p}\right), \tag{1}$$

where

C_p is the capacitance of the test fixture with sample,
C_0 is the capacitance of the test fixture without sample,
R_p is the parallel equivalent resistance of the test fixture with sample and
α is the correction coeffiecient;

$$\tan\delta = \frac{\varepsilon''}{\varepsilon'}. \tag{2}$$

Moreover, the AC conductivity [$\sigma'_{ac}(f)$] is determined using

$$\sigma'_{ac}(f) = \omega\varepsilon_0\varepsilon'', \tag{3}$$

where $\omega = 2\pi f$ is the angular frequency and ε_0 is the permittivity of free space.

3. Results and Discussion

3.1. *Dielectric and electrical properties of uncured epoxy and hardener*

Frequency-dependent dielectric constants (ε') of Bisphenol A-epichlorhydrin (epoxy) and *N*(3-dimethylaminopropyl)-1,3-propylenediamine (hardener) are represented in Fig. 1(a). The dielectric constant values of epoxy are almost frequency-independent over the frequency range of 1 kHz $\leq f \leq$ 0.2 MHz suggesting the absence of any relaxation mechanism. Results can be attributed to lack of enough time for charges of epoxy to build up at the boundaries of conducting surface.[36,37] Moreover, beyond this frequency range, i.e., for 0.2 MHz $\leq f \leq$ 2 MHz, ε' values are found to decrease, which may be due to enhancement in the conduction mechanism of epoxy.[17] Over the frequency range of 1 kHz $\leq f \leq$ 0.3 MHz, the

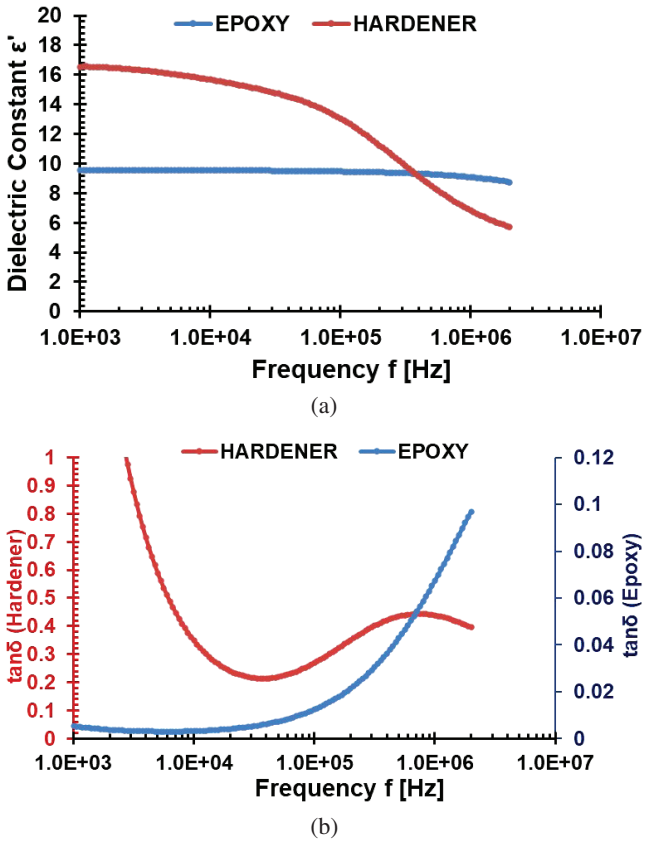

Fig. 1. Frequency-dependent spectra of (a) dielectric constant (ε') and (b) loss tangent (tan δ) for epoxy and hardener.

dielectric constant values of hardener are higher than those of resin, whereas beyond this frequency range a contrary trend is observed. The dielectric constant of hardener exhibited higher values in the lower frequency region which indicates the higher polarity of hardener molecule than the resin.[38] With increase in the frequency, values of ε' of the hardener are found to decrease indicating relaxation mechanism.

Over the frequency range of 1 kHz–0.1 MHz, ε' values of hardener decreased gradually and beyond this frequency range (i.e., 0.1 MHz $\leq f \leq$ 2 MHz) these values decreased at a higher rate.

Frequency-dependent loss tangent (tan δ) spectra for epoxy and hardener are depicted in Fig. 1(b). The tan δ value of uncured epoxy up to around 0.1-MHz frequency is very small (around 0.004) and it starts increasing rapidly with increase in frequency above 0.1 MHz, suggesting a start of relaxation process which could be attributed to the ionic conduction.[39] On the contrary, loss tangent value of hardener is high (1 at 1-kHz frequency) and decreases rapidly with the rise in frequency exhibiting minima at 35.565-kHz frequency, and then it increases exhibiting maxima at 0.75-MHz frequency. Observed high value of tan δ in the low-frequency region is observed and a relaxation peak at 0.75-MHz frequency is due to the dipolar relaxation mechanism. The corresponding dipolar relaxation time is ~0.211 μs ($\tau d = 1/2\pi fd$).

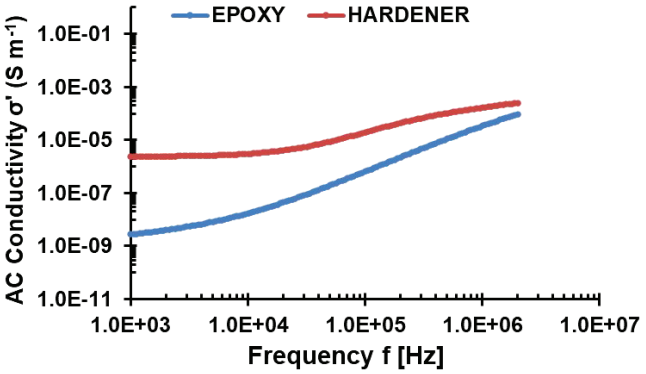

Fig. 2. Frequency-dependent AC conductivity (σ') values for epoxy resin and hardener.

The frequency dependence of AC conductivities (σ'_{ac}) of epoxy and hardener is represented in Fig. 2. At lower frequencies (up to 0.2 MHz for epoxy and up to 20 kHz for hardener), σ'_{ac} exhibits a plateau region, which corresponds to the DC conductivity (σ_{dc}), while at higher frequencies, σ' becomes strongly frequency-dependent and is found to increase with frequency indicating enhancement in the conduction mechanisms of epoxy and hardener.[40] Determined values of DC conductivity for hardener and epoxy are 2.41 $\mu S \cdot m^{-1}$ and 2.81 $nS \cdot m^{-1}$, respectively. Higher value of σ_{dc} of hardener than epoxy can be attributed to the lower value of viscosity of hardener (35,000 cP at 298.15 K)[41] than that of epoxy (50,000 cP at 298.15 K).[42] Results are in agreement with the inverse proportionality relationship $\left(\sigma_{dc}\, \alpha\, \frac{1}{\eta}\right)$ as observed by many researchers.[30,43–46]

3.2. *Dielectric and electrical properties of neat epoxy and nano-epoxy composites*

Frequency-dependent dielectric constant (ε') and loss tangent (tan δ) spectra for neat epoxy and nano-epoxy composites consisting of 1 wt.% of SiO_2, TiO_2, Al_2O_3 and ZnO nanofillers over the frequency range of 1 kHz–2 MHz are shown in Figs. 3(a) and 3(b), respectively. It is observed from Fig. 3(a) that the values of dielectric constant for neat epoxy as well as various nano-epoxy composites decreased marginally with increase in the frequency. At lower frequency, the dipolar functional groups of the neat epoxy are able to orient themselves, whereas at higher frequency the dipolar functional groups are unable to orient. So, orientation polarization in nano-epoxy composites is decreased, causing reduction in dielectric constant values with increase in the frequency.[17,47–50] Also, it is observed from Figs. 1(a) and 3(a) that at 1-kHz frequency, dielectric constant values of hardener, epoxy and neat epoxy are 16.51, 9.51 and 3.30, respectively. Reason for observed order [ε' (neat epoxy) < ε' (epoxy) < ε' (hardener)] could be attributed to the formations of cross-linking networks during curing process, preventing orientation polarization of large molecule.

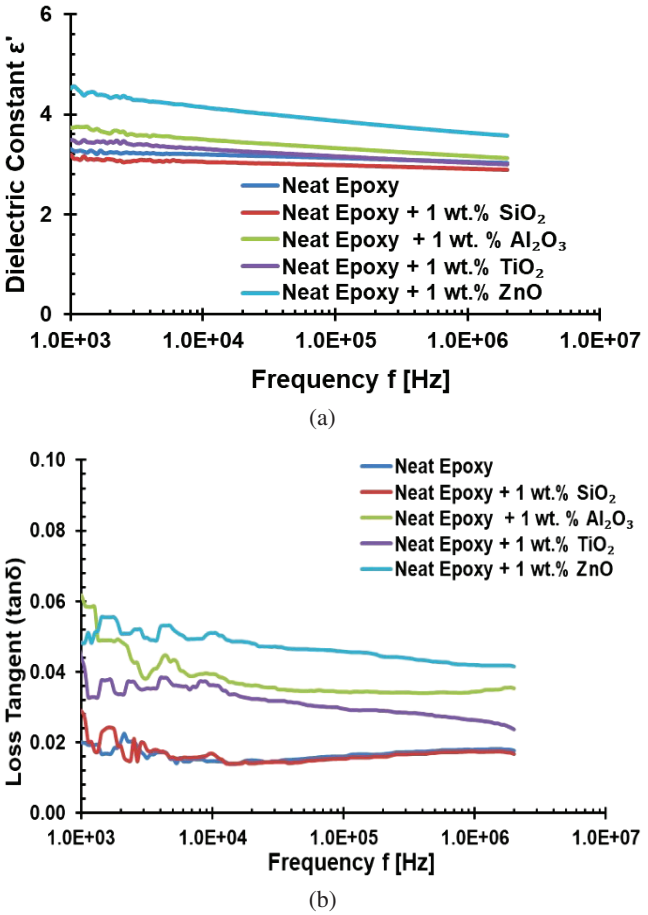

Fig. 3. Frequency-dependent spectra of (a) dielectric constant (ε') and (b) loss tangent (tan δ) for neat epoxy and nano-epoxy composites.

As can be seen from Fig. 3(a), for nano-epoxy composites consisting of TiO_2, Al_2O_3 and ZnO nano-fillers, the dielectric constant values are higher than those of neat epoxy composite, whereas for the nano-epoxy composite of SiO_2 nano-filler, the dielectric constant values are marginally lower than those of neat composite. Results confirmed that the introduction of nano-fillers has influenced the structural arrangement of neat epoxy resin through chemical bindings of the neat epoxy composite causing hindrance to the mobility of dipolar groups in neat epoxy.[51] Reported values of static dielectric constant of SiO_2, ZnO, Al_2O_3 and TiO_2 nano-powders are 4, 8, 10 and 90, respectively, at 300.15-K temperature.[18,52] Static dielectric constant of neat epoxy in this investigation at the same temperature is 3.02. Therefore, it is expected that the dielectric constant of the nano-epoxy composites should be in the order of ($TiO_2 > Al_2O_3 > ZnO > SiO_2$). However, the observed dielectric constants of the nano-filler-loaded epoxy resin are in the order of ε' (ZnO) > ε' (Al_2O_3) > ε' (TiO_2) > ε' (SiO_2) (Fig. 4). This clearly suggests that the structure of epoxy resin changes drastically depending upon the type of nano-filler introduced in the polymer matrix of neat epoxy. This is mainly due to the constraint in the mobility of polymer

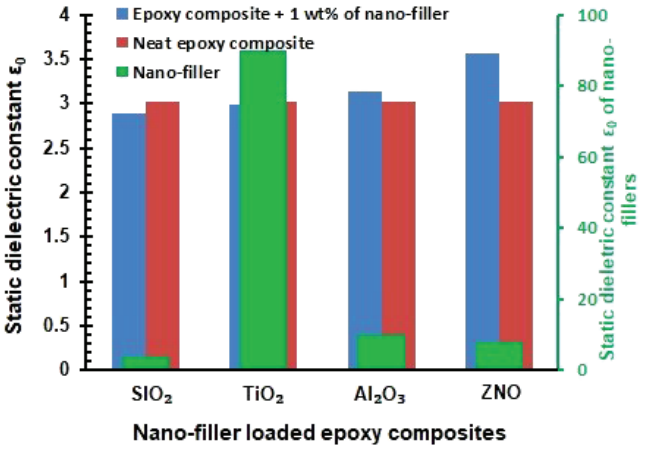

Fig. 4. Comparison of values of static dielectric constant (ε_0) of neat epoxy, nano-epoxy composites and nano-fillers.

chains in nano-epoxy composites due to the interaction process between nano-filler surfaces and polymer chain.[16]

From the frequency-dependent loss tangent (tan δ) spectra as shown in Fig. 3(b), it can be observed for SiO_2- and Al_2O_3-loaded nano-epoxy composites that the values of tan δ are somewhat increased with increase in the frequency which is identical to that of neat epoxy. Whereas in ZnO- and TiO_2-loaded nano-epoxy composites, the tan δ values show marginal but continuous decrease with increase in the frequency and are not identical to those of neat epoxy which may be due to the presence of a significant number of nano-fillers in the system which influences the electrical conductivity mechanism in the nano-epoxy composite.[16,44]

Frequency-dependent AC conductivity (σ'_{ac}) spectra for the neat epoxy and nano-epoxy composites are depicted in Fig. 5(a). Results indicate that the presence of TiO_2, Al_2O_3 and ZnO nano-fillers produces strong influence on the AC conductivity of neat epoxy, but it remains unaltered in the presence of SiO_2 nano-filler. It has been observed from Fig. 5(a) that AC conductivity values are increased with an increase in frequency for all the epoxy composites. Increase in AC conductivity in higher frequency region indicates the presence of mobile charge carries which are sufficiently free to respond to the change in the applied electric field. The conductivity patterns demonstrated a frequency-independent plateau in the low-frequency region (1 kHz $\leq f \leq$ 50 kHz) due to electrode polarization (EP) mechanism and exhibited dispersion at higher frequencies (50 kHz $\leq f \leq$ 2 MHz).

For all prepared nano-epoxy composites, AC conductivity spectra obey the universal dynamic response (UDR) expressed by Jonscher's power law illustrated in the following equation[53–55]:

$$\sigma'_{ac} = \sigma_0 + Af^n, \quad (4)$$

where the constants A and n are pre-exponential factor and the fractional exponents, respectively, and σ_0 corresponds to

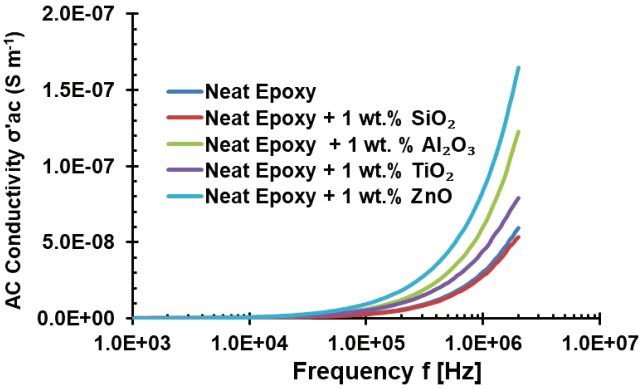

(a)

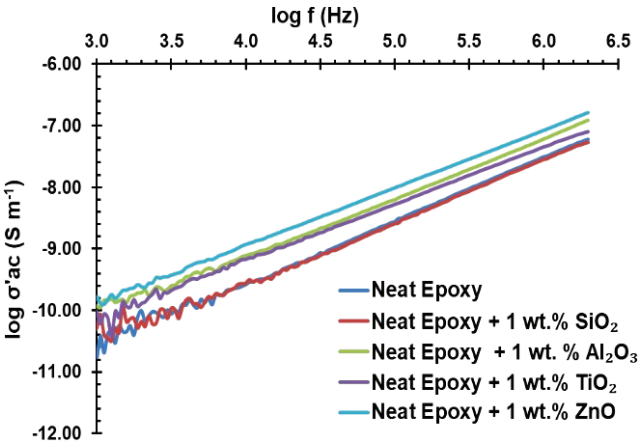

(b)

Fig. 5. (a) Frequency-dependent AC conductivity (σ') spectra and (b) plot of log(σ') versus log(f) for verification of Jonscher's power law.

the frequency-independent plateau, usually identified as the DC conductivity of the material. Analyzing the plot of log(σ') versus log(f) [Fig. 5(b)], where σ_0 values are much less than those of σ'_{ac}, Eq. (4) can be simplified as

$$\sigma'_{ac} = Af^n. \tag{5}$$

Evaluated values of coefficient A and n by fitting the experimental points of Fig. 5(b) in Eq. (5) are reported in Table 1. Values of the fractional exponent (n) are less than 1, indicating that neat epoxy and nano-epoxy composites exhibited random charge conducting paths across the polymer matrices that may or may not intersect each other.[56]

3.3. *FTIR spectroscopic characterization*

In order to understand the actual chemical changes, the nature of bonding and interaction mechanism between the nano-fillers and the neat epoxy material, the structural chemistry of nano-epoxy composites was examined through

Table 1. Evaluated parameters of Jonscher's power law for neat epoxy and nano-epoxy composites.

Nano-epoxy composites	Fitting parameters	
	n	A ($\times 10^{-14}$)
Neat epoxy	0.9964	3.01
Neat epoxy + 1 wt.% of SiO_2	0.9640	4.11
Neat epoxy + 1 wt.% of TiO_2	0.9156	13.9
Neat epoxy + 1 wt.% of Al_2O_3	0.9243	15.9
Neat epoxy + 1 wt.% of ZnO	0.9347	20.7

FTIR spectrometer. Results of the spectra (in terms of absorbance versus wave number) are represented in Fig. 6. The functional groups associated with neat epoxy and nano-epoxy composites at the respective wave numbers are listed in Table 2. Absorption peak observed at 3300 cm^{-1}, corresponds to the stretching vibrations of –OH (hydroxyl) functional group, which reveals the presence of water molecules on the surface of nano-fillers due to affinity of water molecules, present in atmosphere, with nano-fillers. Nano-fillers interact with water molecules via hydrogen bonding.[57] These hydrogen bonds result in the formation of the strongly bonded primary nano-layer of epoxy resin at the interface region which may have influenced the electrical conductivity[58] in nano-epoxy composites as observed in the AC conductivity spectra. Absorption peaks observed at 1651 cm^{-1} corresponding to the bending vibrations of absorbed water molecules are an additional way to the formation of hydrogen bond between epoxy resin and nano-fillers.[59] Around 1600–1650-cm^{-1} wave numbers region, TiO_2 and Al_2O_3 nano-filler-loaded epoxy composites showed low-intensity dual peaks in contrast to single peak of 1612 cm^{-1} in SiO_2 nano-filler-loaded and 1651 cm^{-1} in ZnO nano-filler-loaded epoxy composites. This split is also observed in neat epoxy resin in the same region but it is broad compared to those of TiO_2 and Al_2O_3 nano-epoxy composites.[60]

Based on the FTIR and dielectric characterizations of neat epoxy, possible cross-linking chemical interaction/reaction between epoxy and hardener is expressed in Fig. 7. Primary amine will react with epoxide group and form secondary amine, which further reacted with epoxied group to form a tertiary amine. Later on, due to catalytic effect of tertiary amine, polyether is formed due to self-polymerization of epoxide group.[61]

3.4. *Mechanical properties characterization*

Hardness number of neat epoxy is compared with nano-epoxy composite loaded with SiO_2, TiO_2, ZnO and Al_2O_3 by 0.5, 1 and 2 wt.% in Fig. 8(a). Anomalous behavior is observed in the hardness of neat epoxy composite when varying weight percentages of nano-fillers are doped into it, comparatively

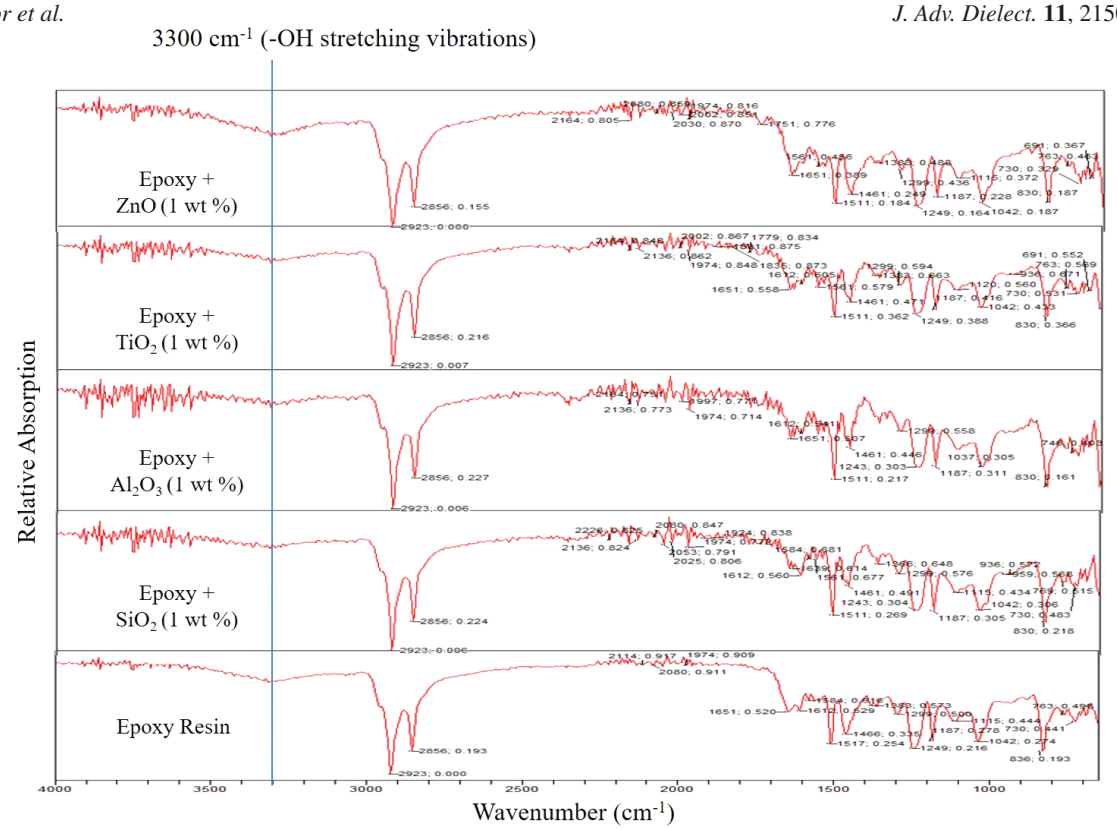

Fig. 6. FTIR spectroscopic results for neat epoxy and nano-epoxy composites.

Table 2. Wave numbers of FTIR peaks and the corresponding functional groups in neat epoxy and nano-epoxy composites.

Wave number (cm^{-1})	Corresponding functional group
3300	O–H stretching vibration
2923	C–H bond stretch of $–CH_3$ group
2856	C–H bond stretch of $–CH_2–$ group
1651	O–H bending vibration
1612	N–H bending of primary amine of $–NH_2$ group
1517, 1466	Ar–C=C–H stretching
1249	Asymmetrical aromatic –C–O– stretch
1187	Asymmetrical aliphatic –C–O– stretch
1042	Stretching –C–O–C– of ethers
836	Stretching –C–O–C– of epoxide group
772	Rocking of $–CH_2$

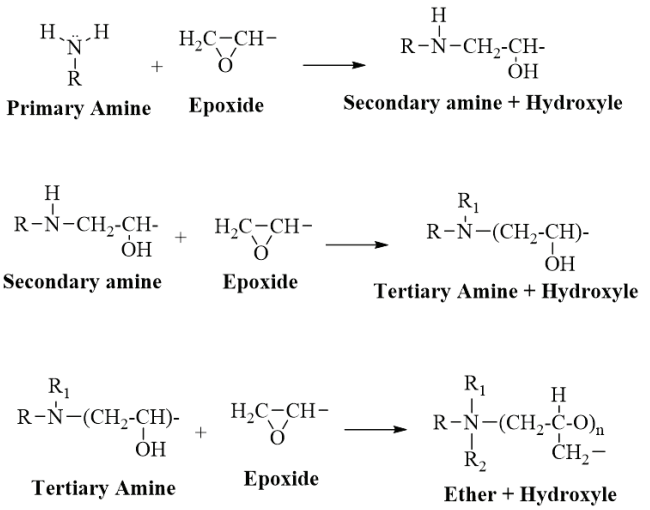

Fig. 7. Possible cross-linking chemical interaction between epoxy and hardener.

higher values of hardness for nano-epoxy composites (except 0.5 wt.% and 2 wt.% of TiO_2 nano-epoxy composites) than those of neat epoxy are observed which suggest uniform dispersion of nano-fillers into neat epoxy composites.[62] Same type of increase in the hardness values of carbon nano-fiber epoxy composites was also observed by Bal.[63] For ZnO nano-filler-loaded epoxy composites, the hardness values are increased gradually with the increase in the wt.% whereas in the case of TiO_2, SiO_2 and Al_2O_3 nano-epoxy composites, the hardness values change anomalously. It can be observed from the spectra that for SiO_2 nano-epoxy composites, hardness values are increased by 23%, 12% and 12% for 0.5, 1 and 12 wt.%, respectively. For TiO_2 nano-epoxy composite,

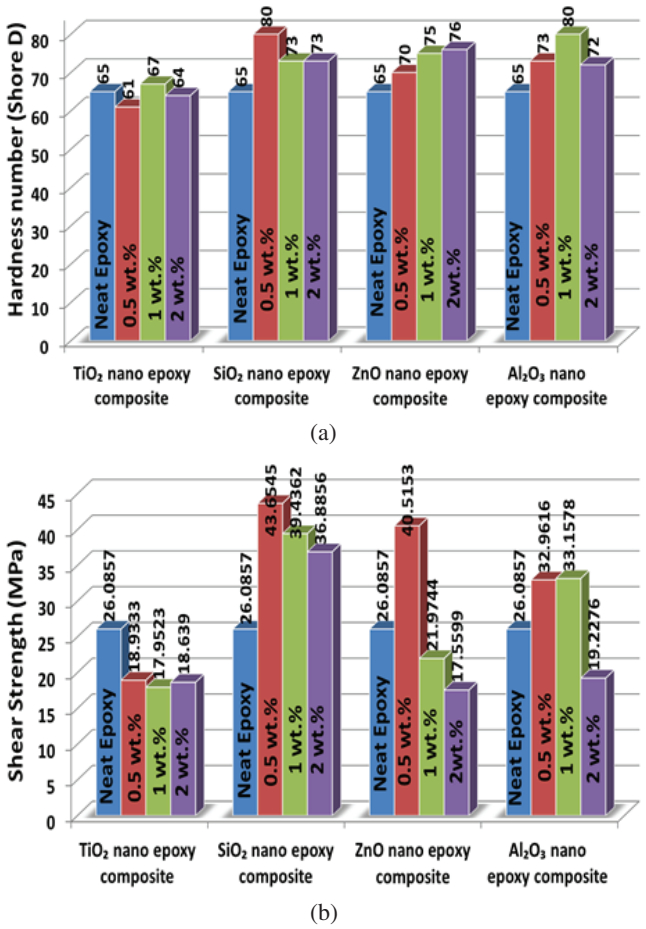

Fig. 8. Comparison of (a) hardness and (b) shear strength of neat epoxy and nano-epoxy composites.

we observed 3% increment in the hardness for 1 wt.%, while for the 0.5 wt.% and 2 wt.% of nano-fillers decrements in hardness value by 6% and 1% were observed, respectively. For ZnO nano-filler-loaded epoxy composites, 7%, 15% and 16% increases in the hardness value are observed for 0.5, 1 and 2 wt.%, respectively. Addition of 0.5, 1 and 2 wt.% of Al_2O_3 nano-filler into neat epoxy led to about 12%, 23% and 10% increases in the hardness, respectively. Measured values of shear strength of neat epoxy are compared with nano-epoxy composites in Fig. 8(b). Anomalous behavior is also observed in shear strength value of neat epoxy composite when varying wt.% of nano-fillers are doped into it. Shear strength of neat epoxy is increased by 67%, 51% and 41% when 0.5-, 1- and 2-wt.% SiO_2 nano-fillers are doped into it, respectively. While the addition of 0.5, 1 and 2 wt.% of TiO_2 nano-fillers into neat epoxy composites resulted in the decrements of 27%, 31% and 28% in the shear strength. For ZnO nano-epoxy composites, shear strength is increased by 55% for 0.5 wt.%, whereas decrements of 15% and 32% are observed for 1 wt.% and 2 wt.%, respectively. However, the addition of 0.5 wt.% and 1 wt.% of Al_2O_3 nano-filler into neat epoxy results in 26% and 27% increments in the shear strength, respectively, and 26% decrement in the shear strength is observed for 2 wt.% of Al_2O_3 nano-filler doped into neat epoxy. It can be concluded from Figs. 8(a) and 8(b) that the mechanical properties such as hardness and shear strength of neat epoxy composite is dependent on the type of the nano-filler and also on the amount of nano-filler doped into it.

Results of hardness and shear strength confirmed their dependence on the bulk internal structure and the surface properties of the nano-fillers, respectively. This can be attributed to microstructural bonds between neat epoxy and nano-fillers which endure the applied force instead of the base matrix.[20,64–68]

3.5. *XRD analysis*

XRD spectra of intensity versus angle of diffraction of SiO_2, TiO_2, Al_2O_3 and ZnO nano-fillers are shown in Fig. 9. It can be observed from the spectra that SiO_2 nano-filler exhibited broad hump near $2\theta = 21.8°$ whereas sharp diffraction peak is absent in the XRD spectra of SiO_2 nano-filler which confirms the amorphous nature of SiO_2 nano-filler.[69–74] For TiO_2 nano-filler, XRD spectra exhibited characteristic peaks at the

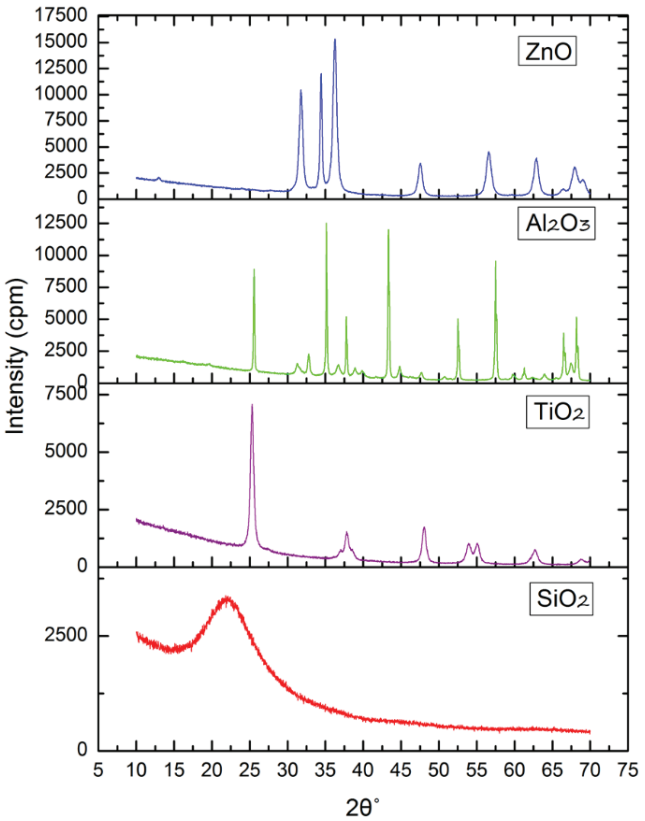

Fig. 9. XRD plot of intensity versus angle of diffraction of nano-fillers.

angles of 25.2°, 37.7°, 38.4°, 47.9°, 53.9°, 55.0°, 62.8° and 68.7° corresponding to TiO_2 anatase phase which are in good agreement with the standard spectrum of TiO2-JCPDS PDF No. 21-1272.[69,75–78] The XRD pattern of Al_2O_3 nano-filler exhibited intensity peaks at 2θ angles of 19.6°, 25.5°, 31.2°, 32.7°, 35.1°, 36.7°, 37.7°, 38.9°, 39.8°, 41.6°, 43.3°, 44.7°, 47.6°, 50.7°, 51.4°, 52.5°, 57.4°, 59.7°, 61.1°, 61.2°, 63.8°, 66.4°, 67.4° and 68.1°, which are in good agreement with the reference XRD pattern of Al_2O_3 (JCPDS File 42-1468) and with other works in the literature.[79–82] Moreover, XRD pattern of ZnO nano-filler exhibited several diffraction peaks at angles of 31.7°, 34.4°, 36.2°, 47.5°, 56.5°, 62.8°, 66.4°, 66.4°, 67.9° and 69° which are in good match with the reference XRD pattern of ZnO-JCPDS PDF No. 01-089-0510.[83–86] On successful matching of the observed characteristic peaks for the nano-fillers with their respective JCPDS [Joint Committee on Powder Diffraction Standard, presently known as the International Centre for Diffraction Data (ICDD)] data as well as by using Scherrer formula, we assure that the fillers have dimensions in the nm range and also conclude that the average particle sizes of SiO_2, TiO_2, Al_2O_3 and ZnO nano-fillers are found to be around 20, 30, 50 and 30 nm, respectively.[69,87]

Figure 10 depicts XRD patterns of the neat epoxy and SiO_2, TiO_2, Al_2O_3 and ZnO nano-epoxy composites. In the XRD spectra of neat epoxy, the existence of two broad peaks is revealed at the angles 18.3° and 42.6° attributed to $C_5H_9NO_2$ and $C_{12}H_{12}N_2$, respectively, which are basically organic components of neat epoxy. This confirms the cross-linked network between epoxy and hardener and also the amorphous nature of neat epoxy.[88–91] It can be seen from the figure that all nano-composites showed same XRD trend similar to that of neat epoxy. All characteristic peaks of TiO_2, ZnO and Al_2O_3 nano-fillers are not recorded in their respective nano-epoxy composite XRD patterns, however, several characteristic peaks were recorded at the same diffraction angle but with different peak intensities, i.e., in TiO_2 nano-epoxy composite one peak at an angle $2\theta = 25.2°$, in Al_2O_3 epoxy nano-composite three peaks at the angles $2\theta = 44.7°$, 57.4° and 67.4°, while in ZnO epoxy nano-composite three peaks at the angles $2\theta = 31.7°$, 34.4° and 36.2°.

The enlarged views of XRD patterns of TiO_2, Al_2O_3 and ZnO nano-filler and nano-epoxy composites are shown in Figs. 11–13, respectively. It is clearly observed from comparison of Fig. 9 and Figs. 11–13 that in epoxy nano-composite all subsequent peaks are at their respective 2θ locations but intensities of their respective peaks are quite small in nano-epoxy composite. This decrease in intensity is expected as small amount of nano-filler was added in neat epoxy.[69,88,89,92,93] Presence of these peaks without change in position in epoxy

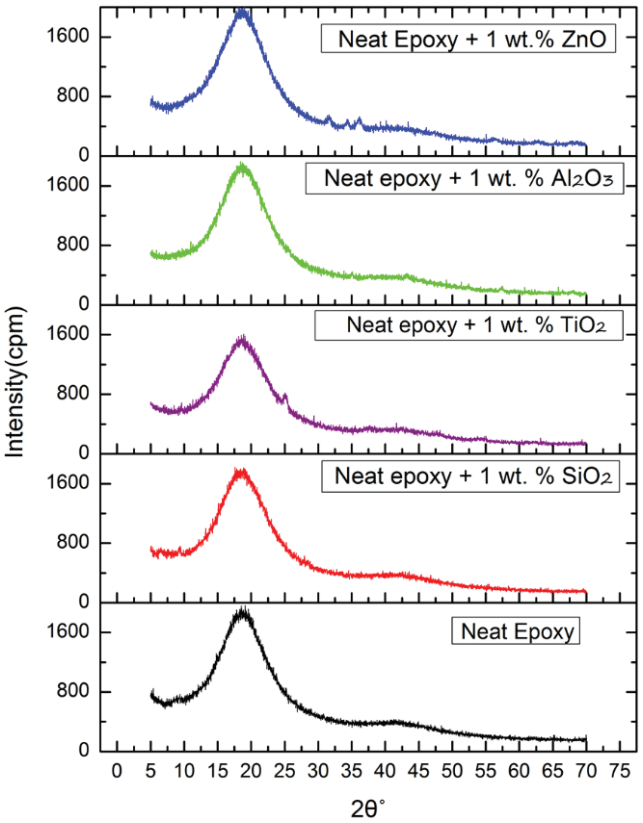

Fig. 10. XRD plot of intensity versus angle of diffraction of neat epoxy and nano-epoxy composites.

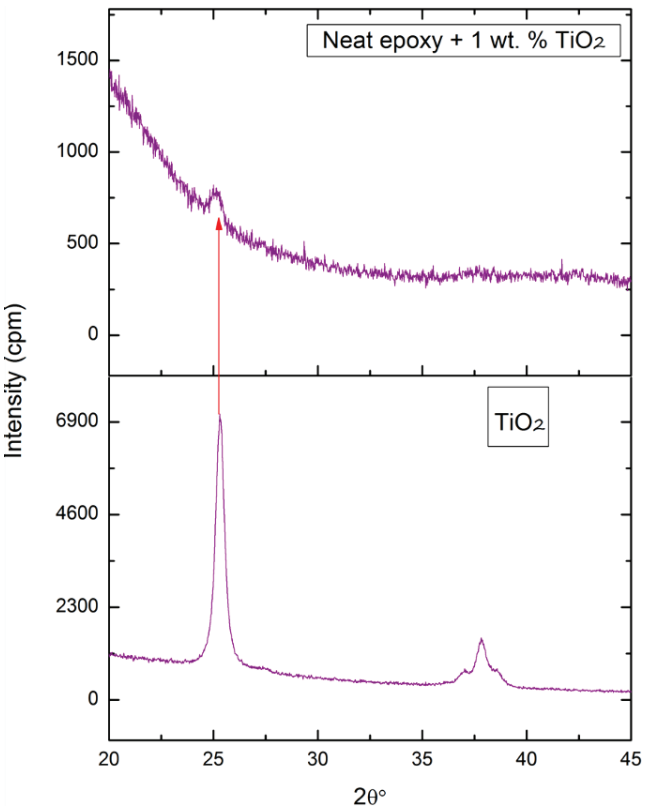

Fig. 11. Enlarged view plot of intensity versus angle of diffraction of TiO_2 nano-filler.

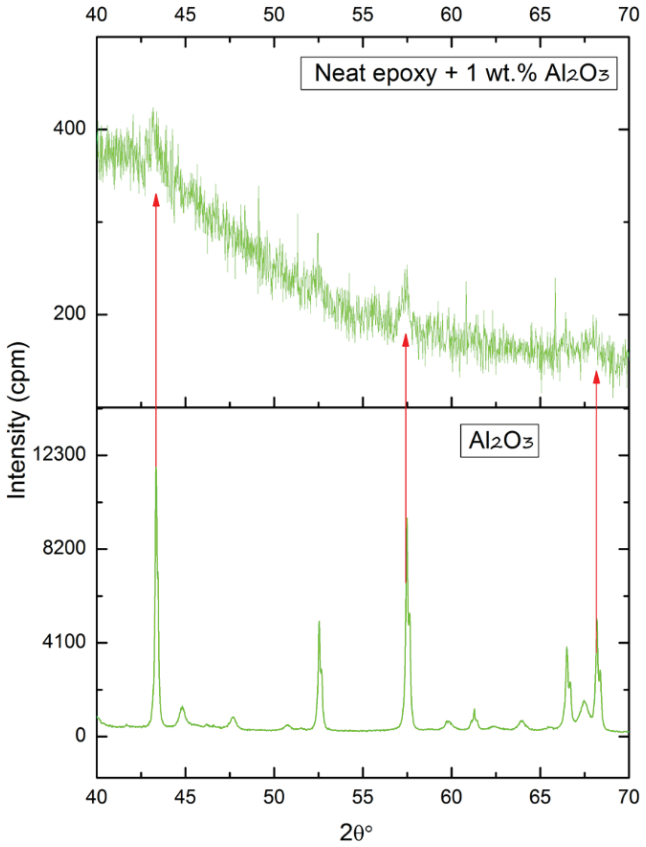

Fig. 12. Enlarged view plot of intensity versus angle of diffraction of Al_2O_3 nano-filler.

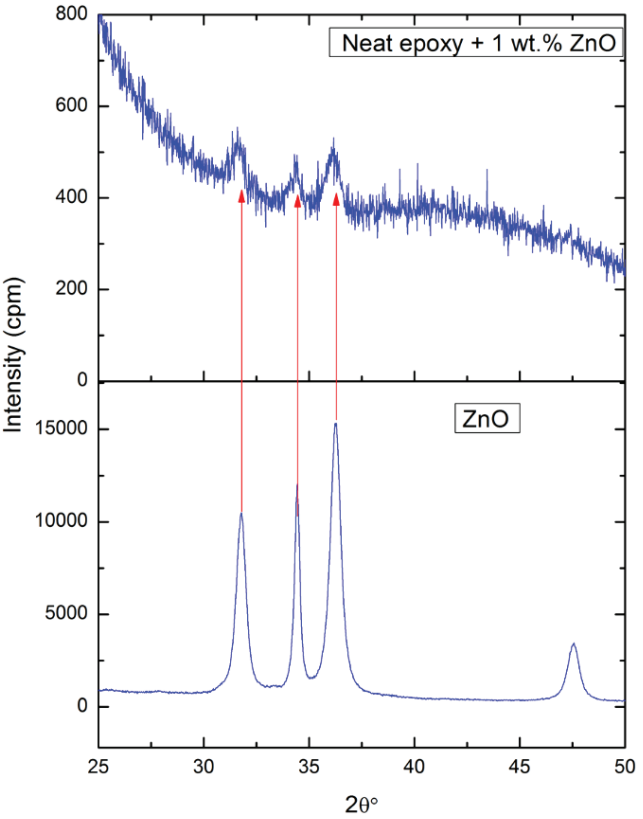

Fig. 13. Enlarged view plot of intensity versus angle of diffraction of ZnO nano-filler.

nano-composite confirms the homogenous and cluster-free dispersion of nano-filler in the entire epoxy matrix.[91]

4. Conclusions

Study of dielectric, electrical and mechanical properties of epoxy, hardener and inorganic nano-filler-loaded epoxy composites is carried out in this work at a constant temperature of 300.15 K. The dipolar relaxation process was observed in hardener, while no such relaxation was found in epoxy over the frequency range of measurement. Larger value of conductivity of hardener is found compared to epoxy, exhibiting the inverse relationship of DC conductivity with viscosity. Effects of adding 1-wt.% inorganic nano-fillers on the dielectric and electrical properties of neat epoxy composites are observed. Nonlinear variation in the static dielectric constant of neat epoxy composites due to doping of different inorganic nano-fillers can be attributed to the constraint in the mobility of polymer chains as well as the interaction between nano-filler surfaces and the polymer chain. Moreover, the structural characterization of inorganic nano-filler-loaded epoxy composite is carried out using FTIR technique. Change in the chemical structure of neat epoxy composite due to inclusion of inorganic nano-filler is observed from the absorption peaks, and a possible interaction between epoxy and hardener is also proposed. FTIR spectra of nano-epoxy composites exhibited the formation of hydrogen bond between epoxy resin and nano-fillers via hydroxyl group of water molecules present in atmosphere. Evident effect of adding nano-fillers of varying wt.% on the mechanical properties of epoxy composites is observed in terms of anomalous variations in the shear strength and hardness. Results can be attributed to the bulk internal structure and the surface properties of nano-fillers. Average particle sizes of SiO_2, TiO_2, Al_2O_3 and ZnO nano-fillers have been determined from XRD traces which are found to be 20, 30, 50 and 30 nm, respectively. Moreover, in the XRD traces, characteristic peaks of nano-fillers were also observed in the corresponding nano-epoxy composite at the same 2θ positions with reduced intensity suggesting cluster-free dispersion of nano-filler in the epoxy composites.

Acknowledgments

Authors are thankful to the funding agency DST, New Delhi for providing financial assistance, through the DST-FIST Projects (SR/FST/PSI-001/2006 and SR/FST/PSI-198/2014). Funding provided by UGC, New Delhi through DRS-SAP Program Grants [Nos. F.530/10/DRS/2010 (SAP-1) and F.530/17/DRS-II/2018 (SAP-1)] is also gratefully

acknowledged. Authors are also thankful to Prof. P. N. Gajjar, Head, Department of Physics, University School of Sciences, Gujarat University, Ahmedabad for his constant encouragement.

References

[1]Z. Wang, M. Yang, Y. Cheng, J. Liu, B. Xiao, S. Chen, J. Huang, Q. Xie, G. Wu and H. Wu, Dielectric properties and thermal conductivity of epoxy composites using quantum-sized silver decorated core/shell structured alumina/polydopamine, *Compos. A, Appl. Sci. Manuf.* **118**, 302 (2019).

[2]L. Fang, C. Wu, R. Qian, L. Xie, K. Yang and P. Jiang, Nano–micro structure of functionalized boron nitride and aluminum oxide for epoxy composites with enhanced thermal conductivity and breakdown strength, *RSC Adv.* **4**, 21010 (2014).

[3]M. Khan, A. A. Khurram, T. Li, T. Zhao, T. Subhani, I. H. Gul, Z. Ali and V. Patel, Synergistic effect of organic and inorganic nano fillers on the dielectric and mechanical properties of epoxy composites, *J. Mater. Sci. Technol.* **34**, 2424 (2018).

[4]Z. Wang, Y. Cheng, H. Wang, M. Yang, Y. Shao, X. Chen and T. Tanaka, Sandwiched epoxy–alumina composites with synergistically enhanced thermal conductivity and breakdown strength, *J. Mater. Sci.* **52**, 4299 (2017).

[5]T. K. B. Sharmila, J. V. Antony, M. P. Jayakrishnan, P. M. S. Beegum and E. T. Thachil, Mechanical, thermal and dielectric properties of hybrid composites of epoxy and reduced graphene oxide/iron oxide, *Mater. Des.* **90**, 66 (2016).

[6]M. Donnay, S. Tzavalas and E. Logakis, Boron nitride filled epoxy with improved thermal conductivity and dielectric breakdown strength, *Compos. Sci. Technol.* **110**, 152 (2015).

[7]Y.-J. Wan, L.-C. Tang, L.-X. Gong, D. Yan, Y.-B. Li, L.-B. Wu, J.-X. Jiang and G.-Q. Lai, Grafting of epoxy chains onto graphene oxide for epoxy composites with improved mechanical and thermal properties, *Carbon* **69**, 467 (2014).

[8]J. Li, Z. Wu, C. Huang and L. Li, Multiscale carbon nanotube-woven glass fiber reinforced cyanate ester/epoxy composites for enhanced mechanical and thermal properties, *Compos. Sci. Technol*. **104**, 81 (2014).

[9]Y.-H. Zhao, Y.-F. Zhang, S.-L. Bai and X.-W. Yuan, Carbon fibre/graphene foam/polymer composites with enhanced mechanical and thermal properties, *Compos. B, Eng.* **94**, 102 (2016).

[10]T. Zhou, X. Wang, X. Liu and D. Xiong, Improved thermal conductivity of epoxy composites using a hybrid multi-walled carbon nanotube/micro-SiC filler, *Carbon* **48**, 1171 (2010).

[11]R. K. Nayak, K. K. Mahato and B. C. Ray, Water absorption behavior, mechanical and thermal properties of nano TiO_2 enhanced glass fiber reinforced polymer composites, *Compos. A, Appl. Sci. Manuf.* **90**, 736 (2016).

[12]Y. K. Wang, L. Chen and Z. W. Xu, Effect of various nanoparticles on friction and wear properties of glass fiber reinforced epoxy composites, *Adv. Mater. Res.* **4**, 1106 (2011).

[13]T. Tanaka, Dielectric nanocomposites with insulating properties, *IEEE Trans. Dielectr. Electr. Insul.* **12**, 914 (2005).

[14]P. Gonon and A. Boudefel, Electrical properties of epoxy/silver nanocomposites, *J. Appl. Phys.* **99**, 24308 (2006).

[15]S. Singha and M. J. Thomas, Permittivity and tan delta characteristics of epoxy nanocomposites in the frequency range of 1 MHz-1 GHz, *IEEE Trans. Dielectr. Electr. Insul.* **15**, 2 (2008).

[16]J. C. Fothergill, J. K. Nelson and M. Fu, Dielectric properties of epoxy nanocomposites containing TiO_2, Al_2O_3 and ZnO fillers, *Proc. 17th Annu. Meeting IEEE Lasers Electro-Optics Society* (2004), pp. 406–409.

[17]S. Singha and M. J. Thomas, Dielectric properties of epoxy nanocomposites, *IEEE Trans. Dielectr. Electr. Insul.* **15**, 12 (2008).

[18]I. Plesa, Dielectric spectroscopy of epoxy resin with and without inorganic nanofillers, *J. Adv. Res. Phys.* **1**, 011011 (2017).

[19]B. Ramezanzadeh, M. M. Attar and M. Farzam, Effect of ZnO nanoparticles on the thermal and mechanical properties of epoxy-based nanocomposite, *J. Therm. Anal. Calorim.* **103**, 731 (2010).

[20]C.-K. Lam, H. Cheung, K. Lau, L. Zhou, M. Ho and D. Hui, Cluster size effect in hardness of nanoclay/epoxy composites, *Compos. B, Eng.* **36**, 263 (2005).

[21]S. Thakor, V. A. Rana and H. P. Vankar, Dielectric spectroscopy of SiO_2, ZnO-nanoparticle loaded epoxy resin in the frequency range of 20 Hz to 2 MHz, *AIP Conf. Proc.* **1837**, 040025 (2017).

[22]S. G. Thakor, V. A. Rana and H. P. Vankar, Dielectric characterization of TiO_2, Al_2O_3-nanoparticle loaded epoxy resin, *AIP Conf. Proc.* **1953**, 050049 (2018).

[23]S. G. Thakor, V. A. Rana and H. P. Vankar, Dielectric spectroscopy of mixed nanoparticle loaded epoxy resin, *Int. J. Sci. Res. Rev.* **7**, 426 (2018).

[24]D. M. Marquis, E. Guillaume and C. Chivas-Joly, *Nanocomposites and Polymers with Analytical Methods*, Chapter 11 (InTechOpen, 2011), pp. 261–284.

[25]B. Wetzel, F. Haupert and M. Q. Zhang, Epoxy nanocomposites with high mechanical and tribological performance, *Compos. Sci. Technol.* **63**, 2055 (2003).

[26]C. B. Ng, L. S. Schadler and R. W. Siegel, Synthesis and mechanical properties of TiO_2-epoxy nanocomposites, *Nanostruct. Mater.* **12**, 507 (1999).

[27]M. N. Bin Zainal, Polymer layered silicates nanocomposite: PLS nanocomposite, Thesis, Universitat Politècnica de Catalunya (2015).

[28]J. R. Ugal and M. E. Abd Al-Fattah, Preparation of epoxy nanocomposites and studying their mechanical, thermal and morphology properties, *J. Kerbala Univ*. **8**, 94 (2015).

[29]Y. Sun, Z. Zhang, K. Moon and C. P. Wong, Glass transition and relaxation behavior of epoxy nanocomposites, *J. Polym. Sci. B, Polym. Phys.* **42**, 3849 (2004).

[30]V. A. Rana, K. N. Shah, H. P. Vankar and C. M. Trivedi, Dielectric spectroscopic study of the binary mixtures of amino silicone oil and methyl ethyl ketone in the frequency range of 100 Hz to 2 MHz at 298.15 K temperature, *J. Mol. Liq.* **271**, 686 (2018).

[31]Keysight Technologies, Keysight E4980A/A Precision LCR Meter Keysight E4980A/AL, Data Sheet (2017).

[32]Keysight Technologies, Keysight 16451B Dielectric Test Fixture, Operation and Service Manuel (2008).

[33]Bureau of Indian Standards, IS 13360-5-11: Plastics — Methods of Testing, Part 5: Mechanical Properties, Section 11: Determination of Indentation Hardness of Plastics by Means of Durometer (Shore Hardness), Indian Standard, Petroleum, Coal, and Related Products, Plastics (1992).

[34]Bureau of Indian Standards, IS 2036: Phenolic Laminated Sheets: Specification, Indian Standard (1995).

[35]The Krishnan Group/Wilcox 132, University of Washington, Rigaku XRD-System Instruction Manual v4/19/03 (2019), http://depts.washington.edu/kkgroup/facilities/PDF/InstructionManualPDF.pdf.

[36]V. A. Rana and T. R. Pandit, Dielectric spectroscopic and molecular dynamic study of aqueous solutions of paracetamol, *J. Mol. Liq.* **290**, 111203 (2019).

[37]P. B. Macedo, The role of ionic diffusion in polarisation in vitreous ionic conductors, *Phys. Chem. Glasses* **13**, 171 (1972).

[38]A. Kyritsis, P. Pissis and J. Grammatikakis, Dielectric relaxation spectroscopy in poly (hydroxyethyl acrylates)/water hydrogels, *J. Polym. Sci. B, Polym. Phys.* **33**, 1737 (1995).

[39]H. P. Vankar and V. A. Rana, Electrode polarization and ionic conduction relaxation in mixtures of 3-bromoanisole and 1-propanol in the frequency range of 20 Hz to 2 MHz at different temperatures, *J. Mol. Liq.* **254**, 216 (2018).

[40]E. Tuncer, I. Sauers, D. R. James, A. R. Ellis, M. P. Paranthaman, T. Aytuğ, S. Sathyamurthy, K. L. More, J. Li and A. Goyal, Electrical properties of epoxy resin based nano-composites, *Nanotechnology* **18**, 025703 (2006).
[41]D. Evans and S. J. Canfer, *Advances in Cryogenic Engineering Materials*, Chapter 46 (Springer, Boston, 2000), pp. 361–368.
[42]Y. A. Tajima, Monitoring cure viscosity of epoxy composite, *Polym. Compos.* **3**, 162 (1982).
[43]D. Kumar, A. Singh and P. S. Tarsikka, Interrelationship between viscosity and electrical properties for edible oils, *J. Food Sci. Technol.* **50**, 549 (2013).
[44]R. J. Sengwa, S. Choudhary and P. Dhatarwal, Characterization of relaxation processes over static permittivity frequency regime and compliance of the Stokes-Einstein-Nernst relation in propylene carbonate, *J. Mol. Liq.* **225**, 42 (2017).
[45]J. Kallweit, Relationship between viscosity and direct current conductivity in PVC, *J. Polym. Sci. A-1, Polym. Chem.* **4**, 337 (1966).
[46]J. Świergiel, L. Bouteiller and J. Jadżyn, Compliance of the Stokes–Einstein model and breakdown of the Stokes–Einstein–Debye model for a urea-based supramolecular polymer of high viscosity, *Soft Matter* **10**, 8457 (2014).
[47]S. Suresh, P. Nisha, P. Saravanan, K. Jayamoorthy and S. Karthikeyan, Investigation of the thermal and dielectric behavior of epoxy nano-hybrids by using silane modified nano-ZnO, *Silicon* **10**, 1291 (2018).
[48]L. D. Zhang, H. F. Zhang, G. Z. Wang, C. M. Mo and Y. Zhang, Dielectric behaviour of nano-TiO_2 bulks, *Phys. Status Solidi* **157**, 483 (1996).
[49]L. M. Levinson and H. R. Philipp, AC properties of metal-oxide varistors, *J. Appl. Phys.* **47**, 1117 (1976).
[50]J. K. Nelson and J. C. Fothergill, Internal charge behaviour of nanocomposites, *Nanotechnology* **15**, 586 (2004).
[51]K. A. Mauritz, Dielectric relaxation studies of ion motions in electrolyte-containing perfluorosulfonate ionomers: 4: Long-range ion transport, *Macromolecules* **22**, 4483 (1989).
[52]Y. Yang, W. Guo, X. Wang, Z. Wang, J. Qi and Y. Zhang, Size dependence of dielectric constant in a single pencil-like ZnO nanowire, *Nano Lett.* **12**, 1919 (2012).
[53]A. K. Jonscher, The 'universal' dielectric response, *Nature* **267**, 673 (1977).
[54]A. K. Jonscher, Dielectric relaxation in solids, *J. Phys. D, Appl. Phys.* **32**, R57 (1999).
[55]Z. M. Elimat, M. S. Hamideen, K. I. Schulte, H. Wittich, A. De la Vega, M. Wichmann and S. Buschhorn, Dielectric properties of epoxy/short carbon fiber composites, *J. Mater. Sci.* **45**, 5196 (2010).
[56]B. M. Greenhoe, M. K. Hassan, J. S. Wiggins and K. A. Mauritz, Universal power law behavior of the AC conductivity versus frequency of agglomerate morphologies in conductive carbon nanotube-reinforced epoxy networks, *J. Polym. Sci. B, Polym. Phys.* **54**, 1918 (2016).
[57]C. Zhang, R. Mason and G. Stevens, Preparation, characterization and dielectric properties of epoxy and polyethylene nanocomposites, *IEEJ Trans. Fundam. Mater.* **126**, 1105 (2006).
[58]Y. Cao and P. C. Irwin, The electrical conduction in polyimide nanocomposites, *Proc. 2003 Annu. Report Conf. Electrical Insulation and Dielectric Phenomena* (2003), pp. 116–119.
[59]H. Alamri and I. M. Low, Effect of water absorption on the mechanical properties of nano-filler reinforced epoxy nanocomposites, *Mater. Des.* **42**, 214 (2012).
[60]M. Kozako, Y. Ohki, M. Kohtoh, S. Okabe and T. Tanaka, Preparation and various characteristics of epoxy/alumina nanocomposites, *IEEJ Trans. Fundam. Mater*. **126**, 1121 (2006).
[61]M. Rajaei, N. K. Kim, S. Bickerton and D. Bhattacharyya, A comparative study on effects of natural and synthesised nano-clays on the fire and mechanical properties of epoxy composites, *Compos. B, Eng.* **165**, 65 (2019).
[62]D. Bazrgari, F. Moztarzadeh, A. A. Sabbagh-Alvani, M. Rasoulianboroujeni, M. Tahriri and L. Tayebi, Mechanical properties and tribological performance of epoxy/Al_2O_3 nanocomposite, *Ceram. Int*. **44**, 1220 (2018).
[63]S. Bal, Experimental study of mechanical and electrical properties of carbon nanofiber/epoxy composites, *Mater. Des.* **31**, 2406 (2010).
[64]S. Mosalman, S. Rashahmadi and R. Hasanzadeh, The effect of TiO_2 nanoparticles on mechanical properties of poly methyl methacrylate nanocomposites, *Int. J. Eng. Trans. B, Appl.* **30**, 807 (2017).
[65]T. Ngo, M. Ton-That, S. V. Hoa and K. C. Cole, Reinforcing effect of organoclay in rubbery and glassy epoxy resins, part 1: Dispersion and properties, *J. Appl. Polym. Sci.* **107**, 1154 (2008).
[66]J. Sanes, F. J. Carrión and M. D. Bermúdez, Effect of the addition of room temperature ionic liquid and ZnO nanoparticles on the wear and scratch resistance of epoxy resin, *Wear* **268**, 1295 (2010).
[67]B. P. Chang, H. M. Akil, R. B. M. Nasir, I. Bandara and S. Rajapakse, The effect of ZnO nanoparticles on the mechanical, tribological and antibacterial properties of ultra-high molecular weight polyethylene, *J. Reinf. Plast. Compos.* **33**, 674 (2014).
[68]N. A. Ai, S. I. Hussein, M. K. Jawad and I. A. Al-Ajaj, Effect of Al_2O_3 and SiO_2 nanopartical on wear, hardness and impact behavior of epoxy composites, *Chem. Mater. Res.* **7**, 34 (2015).
[69]A. Takari, A. R. Ghasemi, M. Hamadanian, M. Sarafrazi and A. Najafidoust, Molecular dynamics simulation and thermo-mechanical characterization for optimization of three-phase epoxy/TiO_2/SiO_2 nano-composites, *Polym. Test.* **93**, 106890 (2021).
[70]T. A. Hassan, V. K. Rangari, F. Baker and S. Jeelani, Synthesis of hybrid SiC/SiO_2 nanoparticles and their polymer nanocomposites, *Int. J. Nanosci.* **12**, 1350008 (2013).
[71]F. L. Deepak, G. Gundiah, M. M. Seikh, A. Govindaraj and C. N. R. Rao, Crystalline silica nanowires, *J. Mater. Res.* **19**, 2216 (2004).
[72]R. Nandanwar, P. Singh and F. Z. Haque, Synthesis and characterization of SiO_2 nanoparticles by sol-gel process and its degradation of methylene blue, *Chem. Sci. Int. J.* **5**, 1 (2015).
[73]S. Musić, N. Filipović-Vinceković and L. Sekovanić, Precipitation of amorphous SiO_2 particles and their properties, *Braz. J. Chem. Eng.* **28**, 89 (2011).
[74]S.-H. Xue, H. Xie, H. Ping, Q.-C. Li, B.-L. Su and Z.-Y. Fu, Induced transformation of amorphous silica to cristobalite on bacterial surfaces, *RSC Adv.* **5**, 71844 (2015).
[75]W. Liu and Y. Zhang, Electrical characterization of TiO_2/$CH_3NH_3PbI_3$ heterojunction solar cells, *J. Mater. Chem. A* **2**, 10244 (2014).
[76]K. Thamaphat, P. Limsuwan and B. Ngotawornchai, Phase characterization of TiO_2 powder by XRD and TEM, *Kasetsart J. (Nat. Sci.)* **42**, 357 (2008).
[77]F. Scarpelli, T. Mastropietro, T. Poerio and N. Godbert, *Titanium Dioxide: Material for a Sustainable Environment*, Chapter 3 (InTechOpen, 2018), pp. 57–80.
[78]S. Phromma, T. Wutikhun, P. Kasamechonchung, T. Eksangsri and C. Sapcharoenkun, Effect of calcination temperature on photocatalytic activity of synthesized TiO_2 nanoparticles via wet ball milling sol-gel method, *Appl. Sci.* **10**, 993 (2020).
[79]T. Zaki, K. I. Kabel and H. Hassan, Preparation of high pure α-Al_2O_3 nanoparticles at low temperatures using Pechini method, *Ceram. Int.* **38**, 2021 (2012).
[80]P. A. Prashanth, R. S. Raveendra, R. Hari Krishna, S. Ananda, N. P. Bhagya, B. M. Nagabhushana, K. Lingaraju and H. Raja Naika, Synthesis, characterizations, antibacterial and photoluminescence studies of solution combustion-derived α-Al_2O_3 nanoparticles, *J. Asian Ceram. Soc.* **3**, 345 (2015).
[81]F. R. Feret, D. Roy and C. Boulanger, Determination of alpha and beta alumina in ceramic alumina by X-ray diffraction, *Spectrochim. Acta B, At. Spectrosc.* **55**, 1051 (2000).

[82]T. Zaki, K. I. Kabel and H. Hassan, Using modified Pechini method to synthesize α-Al_2O_3 nanoparticles of high surface area, *Ceram. Int.* **38**, 4861 (2012).
[83]P. Hosseinkhani, A. M. Zand, S. Imani, M. Rezayi and Z. S. Rezaei, Determining the antibacterial effect of ZnO nanoparticle against the pathogenic bacterium, *Shigella dysenteriae* (type 1), *Int. J. Nano Dimens*. **1**, 279 (2011).
[84]P. Bindu and S. Thomas, Estimation of lattice strain in ZnO nanoparticles: X-ray peak profile analysis, *J. Theor. Appl. Phys.* **8**, 123 (2014).
[85]M. Jabeen, M. A. Iqbal, R. V. Kumar, M. Ahmed and M. T. Javed, Chemical synthesis of zinc oxide nanorods for enhanced hydrogen gas sensing, *Chin. Phys. B* **23**, 018504 (2013).
[86]R. Yogamalar, R. Srinivasan, A. Vinu, K. Ariga and A. C. Bose, X-ray peak broadening analysis in ZnO nanoparticles, *Solid State Commun.* **149**, 1919 (2009).
[87]T. Theivasanthi and M. Alagar, Titanium dioxide (TiO_2) nanoparticles XRD analyses: An insight, Preprint, arXiv:1307.1091 [physics.chem-ph] (2013).
[88]S. A. Bello, J. O. Agunsoye, J. A. Adebisi and S. B. Hassan, Effect of aluminium particles on mechanical and morphological properties of epoxy nanocomposites, *APTEFF* **48**, 25 (2017).
[89]R. Khan, M. R. Azhar, A. Anis, M. A. Alam, M. Boumaza and S. M. Al-Zahrani, Facile synthesis of epoxy nanocomposite coatings using inorganic nanoparticles for enhanced thermo-mechanical properties: a comparative study, *J. Coat. Technol. Res.* **13**, 159 (2016).
[90]M. A. Alam, U. A. Samad, E.-S. M. Sherif, A. M. Poulose, J. A. Mohammed, N. Alharthi and S. M. Al-Zahrani, Influence of SiO_2 content and exposure periods on the anticorrosion behavior of epoxy nanocomposite coatings, *Coatings* **10**, 118 (2020).
[91]A. Kumar, K. Kumar, P. K. Ghosh and K. L. Yadav, MWCNT/TiO_2 hybrid nano filler toward high-performance epoxy composite, *Ultrason. Sonochem.* **41**, 37 (2018).
[92]M. Eskandari, M. N. Liavali, R. Malekfar and P. Taboada, Investigation of optical properties of polycarbonate/TiO_2/ZnO nanocomposite: Experimental and DFT calculations, *J. Inorg. Organomet. Polym. Mater.* **30**, 5283 (2020).
[93]A. Mostafaei and F. Nasirpouri, Preparation and characterization of a novel conducting nanocomposite blended with epoxy coating for antifouling and antibacterial applications, *J. Coat. Technol. Res.* **10**, 679 (2013).